Dynamic pH measurement of intracellular pathways using nano-plasmonic assemblies

Kazuki Bando[1], Zhiqiang Zhang[2], Duncan Graham[3], Karen Faulds[3], Katumasa Fujita[1,4,5]* and Satoshi Kawata[1,6]

1. Department of Applied Physics, Osaka University, Yamadaoka, Suita, Osaka 565-0871, Japan
2. CAS Key Lab of Bio-Medical Diagnostics, Suzhou Institute of Biomedical Engineering and Technology, Chinese Academy of Sciences, 215163, Suzhou, China
3. Centre for Molecular Nanometrology, Department of Pure and Applied Chemistry, WestCHEM, University of Strathclyde, Technology and Innovation Centre, 99 George Street, Glasgow, UK
4. Advanced Photonics and Biosensing Open Innovation Laboratory, AIST-Osaka University, Yamadaoka, Suita, Osaka 565-0871, Japan
5. Transdimensional Life Imaging Division, Institute for Open and Transdisciplinary Research Initiatives, Osaka University, Yamadaoka, Suita, Osaka 565-0871, Japan
6. Serendip Research, Yamadaoka, Suita, Osaka 565-0871, Japan

*fujita@ap.eng.osaka-u.ac.jp

Abstract

Plasmonic Ag nano-assemblies moving in a living cell were employed to visualize the spatiotemporal change of intracellular pH by surface-enhanced Raman scattering. Ag nano-assemblies were functionalized by 4-mercaptobenzoic acid (p-MBA) to monitor the variation of the surrounding pH. SERS spectra from the functionalized nano-assemblies that were transported in a cell were measured to estimate the local pH on the pathways travelled by the nano-assemblies. The 3D nanoparticle tracking and the SERS measurements were simultaneously performed to trace the pH dynamics with a spatial accuracy of several tens of nanometers and a temporal resolution of 200 ms, which are sufficient to reveal pH changes associated with intracellular transportation. The pH trajectory of the functionalized nanoparticle can visualize the dynamic change of the chemical environment caused by organelle interactions, such as endosomal trafficking and lysosomal fusion. This breakthrough creates a new paradigm for intracellular

analysis using SERS and reveals new capability for rapid use of SERS in biological analysis.

Introduction

Nano-sized metallic nanoparticles provide an enhanced electro-magnetic field on the metal surface when irradiated by light. This field enhancement effect has been utilized to the harness the optical effects of the particle and adjacent materials and, in particular, light scattering effects. Surface-enhanced Raman scattering (SERS) is very attractive for scientists to allow high-sensitivity molecular analysis based on vibrational spectroscopy.[1-3] In order to utilize the SERS phenomena for analyzing and imaging molecules, the combination of SERS spectroscopy and microscopy have been performed by using metallic nanostructures to observe a sample with nanometer-scale resolution.[4-7]

To expand SERS techniques to nanoimaging from inside a cell, the use of metallic nanoparticles has been proposed in order to provide the distribution of the intracellular materials. Dynamics and distribution of intracellular molecules such as DNA bases, amino acids and proteins have been observed in time and space.[8-11] In addition, to detect intracellular molecules, the functionalization of nanoparticles has been proposed to sense intracellular chemical environments, such as pH. Kneipp et. al. reported a temporal change of pH distribution by using silver nanoparticles coated with para mercaptobenzoic acid (p-MBA)[12] that showed a pH sensitive response in the spectral data. Measurement of pH dysregulation due to pH stress from the extracellular environment was reported by A. Jaworska et al.[13]. Although there are several reports using fluorophores for pH sensing [14,15], SERS based pH sensing avoids photobleaching and autofluorescence from cellular proteins. Monitoring changes in pH allows us to know the parameters of various states of cellular activities such as cell division[16], cell metabolism of tumors[17] and bio synthesis of cytoplasmic constituent and transportation.[18,19] Studies of intracellular pH monitoring or mapping have so far been implemented by illuminating with confocal laser scanning or uniform illumination.[20] The pH measurements in cells reveals whole trends of the cellular state or responses due to the environment.[21,22] However, pH differs between each organelle. The proton gradient is regulated temporally and spatially to maintain the correct environment for normal function and activity. The cellular cytoplasm is segmented into organelles by lipid membranes and the proton ion gradient strictly controlled by ion channels or transporters.[17] Therefore, precise temporal and spatial pH measurements are necessary in order to understand the local cellular dynamics at the single organelle level.

In this paper, we observed the pH dynamics of intracellular transportation in three-dimensions by using Ag nanoparticles functionalized with p-MBA. In our previous report, we introduced metallic nanoparticles into living cells by endocytosis and traced the motion of the particles with measuring SERS spectra.[6,11] We applied this dynamic SERS imaging technique to observe the change of pH around the nanoparticles during the endosomal activities surrounding the nanoparticle under intracellular transportation. This three-dimensional pH tracking technique has potential to understand local phenomena at the single cell organelle level such as the intracellular transportation mechanism.

Result and discussion

Self-assembled nanostructure and functionalization for pH sensing

A self-assembled nanostructure having several nano-gaps was designed for local pH sensing with high sensitivity as illustrated in Fig. 1 A. The nano-gaps create the enhanced electric field and provides strong SERS signals.[23] Firstly, we synthesized Ag nanoparticles with a diameter of 50 nm based on the Lee and Meisel method.[24] The nanoparticles were aggregated in a controlled manner by cross-linking using hexamethylenediamine (HMD).[25] In addition, polyvinylpyrrolidone (PVP) was added in order to prevent excess aggregation. Bovine serum albumin (BSA) was added and adsorbed onto the conjugate to further stabilize the nanoparticles and quench any aggregation. We controlled the aggregation condition for the majority of the particles in order to form aggregates, which was confirmed by SEM (Supporting Information Fig. S1). The majority of the aggregates were dimer (28% of the all nanoparticles), which can increase the signal enhancement[26] with keeping the uptake efficiency relatively high.[27] Although the morphology of the particle that occupies the largest number was still monomeric after the aggregation process, more than 50% were counted as aggregates (dimer, trimmer and larger aggregates). They provide a highly enhanced Raman signal even at an early stage of endocytosis before the nanoparticles would be accumulated at the late endosome or lysosome[4]. Then p-MBA molecules were conjugated onto the nanoparticle assemblies. p-MBA molecules are known to make a self-assembled monolayer on metallic surfaces through the thiol group binding to the metal.[28,29] The size of p-MBA molecules are smaller than other adsorbed molecules or proteins, therefore, p-MBA can enter into the gap to bind to the surface of the nanoparticles and provide highly effective SERS.

We measured SERS spectra from the synthesized p-MBA conjugated Ag nano assemblies in solutions at different pHs. The SERS spectra shown in Fig. 1B were collected from assembled nanoparticles immobilized on a glass substrate. The surface of the glass substrate was positively charged by being coated with 3-aminopropyl-triethoxysilane to adsorb the Ag nano assemblies with a negative charge. The glass substrate was filled with McIlvaine solution and adjusted to a different pH for each measurement. SERS imaging was performed by using a home-built line-illumination Raman microscope.[30,31] The excitation wavelength was 532 nm and the assembled nanoparticles were imaged with a water-immersion 1.27 NA objective lens (60x, Nikon). The pH was altered between 3.0 and 9.0 on the same substrate, and SERS imaging performed on the same area (Supporting Information Fig. S2). 100 SERS measurements were taken at randomly selected spots and the average spectra calculated for each pH condition. Each average SERS spectrum was normalized to the peak intensity at 1590 cm^{-1} which is assigned to the vibration mode of the aromatic ring.[25] As reported in previous literature[32,33], the peak intensity of the carboxylate group (1390 cm^{-1}) and C=O stretching mode (1690 cm^{-1}) showed a pH dependent response (Fig.1 (B)). A calibration curve for pH measurement was obtained by fitting the spectral data with a sigmoidal function (Fig.1 (C)). We confirmed that the SERS of the pH probe was sensitive within the range of pH from 3.0 to 9.0 (pKa 6.05), which covers the typical range of intracellular pH (pH 4.8-8).[33]

Fig. 2A shows the reproducibility of the SERS response of the Ag nano assemblies at pH 4.0 to 8.5. SERS spectra were measured from the immobilized Ag nano assemblies on a glass substrate for pH calculation (Fig.2B). The Ag nano assemblies were immersed in two different pH conditions alternately and the result confirmed that the Ag nano assemblies can be used to measure a temporal change of pH. The reproducibility of the spectrum from each SERS spot during a measurement is necessary to estimate a pH in a cell accurately. The SERS spectrum can be affected by the change in the plasmon resonance of nano assemblies.[34] In our experiment, the error bars in Fig.1C include variations in pH estimation due to the spectrum change. The other factor we should note is the thermal damage of nano assemblies by laser irradiation, which also alters the condition for plasmon resonance. In our experiment, Fig. 2B, which showed the spectrum reproducibly overtime under the different pH conditions, indicates that the laser irradiation did not cause significant laser damage on the nano assemblies during the measurement. Although we did not see a significant spectral difference, setting the appropriate parameter such as size distribution of the nano assemblies and the excitation laser power would be necessary to

maintain reproducibility on the spectral shape.

Time-lapse SERS imaging with line illumination

To observe the pH dynamics in a living cell, we performed time lapse SERS imaging using the same Raman system.[30,31] Fluorescence imaging was also simultaneously performed on the same system. We used HeLa cells as a sample. The cells were incubated with the Ag nano assemblies and culture medium for 6 hours, which was enough for them to be endocytosed and transported inside a cell prior to the measurement.[35] In order to understand the location of Ag nano assemblies in the cells, we used Lyso Tracker Blue (L7527, Thermo Fisher Scientific) to indicate the intracellular lysosomes by fluorescence imaging.

Fig. 3A shows the result of time-lapse SERS and fluorescence imaging of a live HeLa cell. SERS and fluorescence images were obtained every 5.5 sec. The SERS images show the distribution of the intensity of the Raman peak at 1590 cm^{-1}, assigned to the aromatic ring vibration mode of p–MBA. Fig.3B shows the trajectory of an Ag nano assembly in a cell, which is indicated by the white color, recorded every 5.5 sec. The position of the assembly was calculated by 2D Gaussian fitting to the SERS image at 1590 cm^{-1}. The Ag nano assembly moved straight ahead and then turned back the way it traveled halfway during the measurement. This linear motion of the assembly suggests that the Ag nano assembly might be being transported by a motor protein such as kinesin or dynein along the intracellular transportation network of microtubules.[34]

The pH around the nano assembly was calculated from the spectra by using the pH calibration curve (Fig. 3D) at each measured frame and plotted on the trajectory as shown in Fig. 3C. The data shows the pH dynamics of the nano assembly correlated with the time and location in the cell. Initially, the pH was around pH 5.4 for 5 minutes and then the pH decreased suddenly from about 5.4 to 5.1 in 2 minutes. When the sudden pH decrease was observed, it was confirmed that the position of the Ag nano assembly overlapped with a lysosome, as indicated by the fluorescence image in Fig. 3A. This observation implies that the sudden pH change around the Ag nano assembly was due to the fusion of an endosome into a lysosome. Lysosomes are known to maintain a highly acidic pH due to its digestive function in a cell.[35] Since the Ag nano assembly was introduced into the cell through endocytosis, the Ag nano assembly will be enclosed by phospholipid layers.[5] It is known that the typical size of the lysosome is 100-500 nm diameter, and the size increases to 500-1500 nm as a result of membrane fusion.[36] The spatial resolution of

the slit confocal microscopy is 255 nm for x and y directions with using an NA-1.27 objective lens, where the accuracy in localization of nano assembly by 2D Gaussian fitting is ~20 nm. Considering the measurement conditions and simultaneous imaging results of SERS and fluorescence, we propose that this shows that the Ag nano assembly was transported from a late endosome to a lysosome.

Another Ag nano assembly showed a different behavior in terms of motion and pH (Fig. 3E-H), which was obtained under the same experimental condition as the data in Fig. 3A-D. The SERS and fluorescence images indicate that the Ag nano assembly moved with a lysosome. The motion of the Ag nano assembly was well-confined in a limited volume after about 5 minutes of measurement. After that, the Ag nano assembly was found to move in a relatively linear motion. The pH value was mostly below 5.0 during the measurements (Fig. 3G-H). This result indicates that the Ag nano assembly was already enclosed in a lysosome at the beginning of the measurement.

3D particle tracking and SERS sensing

We applied the Ag nano assemblies to 3D nanoparticle tracking and simultaneous SERS measurements in a living HeLa cell (see "Materials and methods" for the detail).[6,11] We used a combination of dual-focus dark-field microscopy and Raman spectroscopy. The dual-focus dark-field image detects an x, y, and z position of a targeted nano assembly and provides feedback to two galvanometer mirrors for lateral scanning and an objective lens mount for axial scanning to keep irradiating the same nano assembly moving in 3D space for continuous SERS measurement. Both the dual-focus dark-field images and SERS spectrum were obtained every 200 ms and the number of total image frames was 500 (see supplementary movie SM1). In this measurement, the functionalized nanoparticles traveled in an area ranging ~1 μm for x, ~ 1.5 μm for y, and 1 μm for the z axis Fig. 4 (A). The spatial resolution for the x-y direction was 350 nm, which is obtained from the full width half maximum of the Gaussian fitting of the dark-field image of the nanoparticle (Fig. S3). The accuracy for the x-y direction and z direction is ±22 nm and ±35 nm respectively.[10]

A 3D pH plot corresponding to the trajectory map is shown in Fig. 4 (B). The pH value was estimated by using the intensity ratio of the 1390 cm^{-1} and 1690 cm^{-1} bands for every single frame and plotted in the 3D space. The pH value was about 4.5 at the start of the measurement and

increased to 5.25. This pH range was in agreement with a transition from late endosome to lysosome[18,19], and the change of pH occurred in the opposite manner to the result shown in Fig.3 (A-D). These facts indicate that the pH increase observed in Fig. 4 (B) is likely due to alkalization by fusing of the vesicle that enclosed the nano assemblies and a vesicle with low pH, implying that a lysosome that contained nano assemblies was fused with an early or a late endosome with a pH higher than the lysosome.[19] The main player in endosomal acidification is the vacuolar ATPase, which consists of two multi-subunit domains, the transmembrane V_0 and the cytoplasmic V_1 and works as a proton pump. It is known that the region of assembly of the two sectors : V_1 and V_0 of the ATPase in late endosome increases after early endosome.[37] The lysosome is then more acidic and it suggests that ATPase works more actively. The ATPase system could temporarily reduce as a whole when the endosome fuses with a lysosome resulting in the detection of the pH increase.

Conclusion

We synthesized a SERS-based pH sensing probe by functionalizing Ag nanoparticles with p-MBA molecules. The nanoparticles were assembled into nano assemblies and the number of the nanoparticles per assembly were controlled for the purpose of measuring the dynamics of intracellular pH. The result of time-lapse SERS imaging with slit-illumination Raman microscopy showed time and location dependent pH changes in a living cell. The simultaneous measurement of fluorescence images of lysosomes and SERS spectra indicated that the decrease in pH was due to the lysosome internalization. We also performed 3D tracking of a nano assembly by SERS measurements and obtained the spatiotemporal variation of pH in a live cell. In this experiment, we observed a decrease of pH around the nano assembly, which can be induced by a fusion process of the lysosome and an endosome.

The homeostasis of intracellular pH is maintained at the organelle level in healthy conditions, but abnormal pH causes various diseases such as cancer[38], Parkinson's and Alzheimer's diseases.[39] Therefore, techniques for time-lapse observation of the pH at the organelle level play an important role in accessing the chemical environment in live cells for processes in the basic life sciences such as proliferation[40], phagocytosis[41], apoptosis[42] and in the clinical medicine arena such as monitoring drug efficacies.[43]

Further extension of the intracellular SERS study can be achieved by developing a multi-modal functionalized SERS probe. Since the band width of the Raman scattering is narrow, several Raman peaks can be detected simultaneously. Therefore, surface modification with molecules sensitive to different parameters can provide multiplex chemical information, such as temperature[44], ion concentration[45] and intermolecular interaction[46], in nanometer-scale environments of a live cell, which is difficult to be performed by fluorescent techniques.

Materials and Methods

Synthesis of 50 nm Ag nanoparticles

The Ag nanoparticles were prepared according to a modified Lee and Meisel's method.[21] To synthesis 22 nm Ag seed nanoparticles, a mixture of 30 mL of glycerol and 40 mL of H_2O in a 100 mL flask was heated up to 95 ºC under vigorous magnetic stirring. Then, 18 mg of silver nitrate dissolved in 1.0 mL of H_2O was added. After 1 min, 2.0 mL of sodium citrate (3%) was added. The reaction mixture was stirred for 2 h at 95 ºC and cooled down to room temperature. The obtained 22 nm Ag seed nanoparticles were used as the seeds to produce 50 nm Ag nanoparticles. In a 60 mL vial, 3.6 mL of H_2O and 1 mL of 1% citrate were added into 27.0 mL of H_2O at room temperature. Then, 1.1 mL of 22 nm Ag nanoparticle solution were added. After 5 min, 230 mL of a mixture diamine silver complex (20 mg silver nitrate in 1 mL water plus 220 mL ammonium hydroxide 28%) together with 18 mL of ascorbic acid solution (7.5 mg) were added. The growth finished after 1 h.

Nanoparticle assembling and functionalization

Nanoparticle assembly and functionalization was carried out according to the modified Pallaoro's protocol[20]. 300 µL of Ag nanoparticles were mixed with 5 µL of HMD (0.4 mg mL^{-1} in deionized water (DI)) waiting for 1 minutes, then adding 50 µL of 1% of PVP in DI and waiting for 1 minute. 150 µL of 2% of BSA was then added and waiting for 15 minutes, followed 10 µL of KCl (50 mM in DI) was added and waiting for 5 minutes. After that, 20 µl of p-MBA (100 µM in methanol) was added followed by 30 µl of KCl (500 mM in DI)) and waiting for 24 hours. After that, the functionalized assembled nanoparticles dispersed solution was centrifuged (4.5 K rpm) for 12 minutes and supernatant solution was removed, followed by adding 300 µL of PBS solution.

SERS observation for pH calibration curve

The Ag nano assemblies were fixed on a glass substrate (P50G-1.5-14-Fl, Mattek). 20% 3-Aminopropyltriethoxysilane (APTS) (KBM-903, Shin Etsu Silicone) was dropped on the glass substrate and after 2 minutes, the APTS was washed and Ag nanoparticle assemblies dispersed solution was dropped. Then after 2 hours, supernatant was washed with DI and the dish was filled

with McIlvaine solution and replaced to different pH solution from 3.0-9.0 for every measurement. SERS imaging was performed with a home-built slit-scanning Raman microscopy (see below). The laser power was 0.3 mW/μm^2 and 50 ms/line.

Sample preparation for Simultaneous imaging of SERS and fluorescence imaging

The cell type used in our study was HeLa cells and, which were cultured on the glass bottom dish in a Dulbecco's modified eagle's medium (DMEM) solution at 37 ºC, 5% CO_2 concentration. 100 μl of the dispersed solution of p-MBA conjugated assembled nanoparticles was incubated 2 hours before the imaging. Lysosome staining was carried out with Lysotracker Blue (Thermo Fisher scientific). 50 nM of Lysotracker Blue was suspended Hanks' Balanced Salt Solution (HBSS) and incubated in the incubator at 37 degree Celsius, 5% CO_2 concentration 30 minutes before the imaging.

Slit-scanning Raman microscopy

Simultaneous imaging of SERS and fluorescence was performed with a home-built slit-scanning Raman microscopy and fluorescence microscopy. A 532 nm CW laser (DPSS Millennia eV, Spectra Physics) was used for SERS excitation. The laser beam was shaped with line-shape by a cylindrical lens. The line-shaped spot was focused on the sample on the stage of a commercial microscopy (Ti, Nikon) by an objective lens (CFI Plan Apo IR 60x WI, Nikon). The back scattered SERS signal was collected as spectra over time with the same objective lens and detected by an EMCCD camera (iXon Ultra, Andor) after pathing through a 532 nm long-pass edge filter (LP03-532RU-25, Semrock) and a spectrophotometer (MK-300, Bunkou-keiki). To obtain a SERS image, the line shaped laser was scanned to the normal axis to the line shaped laser with controlling a galvanometer mirror (710–745825, 000- 3014016, GSI Lumonics). The laser power was 0.3 mW/μm^2 and 50 ms/line. The Raman microscope is equipped with a mercury lamp and a custom-made dichroic mirror (Asahi Spectra) to obtain fluorescence signal of Lyso Tracker Blue and SERS signal simultaneously. The fluorescence signal was detected by a sCMOS camera (Zyla-4.2, Andor).

3D SERS tracking microscopy

3D SERS tracking results were obtained with a home-built slit-scanning Raman microscopy. The system consists of a dual-focused dark-field imaging system and point illumination Raman

microscopy. The laser for SERS excitation and spectrophotometer, objective lens, microscopy body and a detector for SERS signal was the same as the slit-scanning Raman microscopy above. A laser spot was focused on the sample plane on the microscopy body. Two galvanometer mirrors for x and y directions on the sample plane were used to keep the laser focus spot on a specific targeted nanoparticle. The position of the nanoparticle was detected by the dual-focused dark-field imaging system was sent to the controller for the two galvanometer mirrors. A halogen-lamp was used for dark-field illumination through a dark-field condenser (0.8–0.95 N.A., Nikon). The scattering light was collected through two divided optical paths. An imaging lens on one of two optical paths was slightly moved along the optical axis. Two images were formed on an EMCCD camera (iXon Ultra, Andor) with different focal planes. Z position of the nanoparticle was calculated from the ratio of the scattering intensity from the two nanoparticle images and z axis piezo (PI) mounted on the objective lens was kept moving to keep focusing on the nanoparticle according to the ratio value during the tracking measurement.

Conflicts of interest

There are no conflicts to declare.

Acknowledgements

This work was supported by JSPS KAKENHI Grant Number 26000011.

References

1. K. Kneipp, Y. Wang, H. Kneipp, L. T. Perelman, I. Itzkan, R. R. Dasari and M. S. Feld, *Phys. Rev. Lett.*, 1997, **78**, 1667–1670.
2. P. G. Etchegoin and E. C. Le Ru, *Anal. Chem*, 2010, **82**, 2888–2892.
3. C. Lafourcade, K. Sobo, S. Kieffer-jaquinod, J.́rome Garin and F. G. van der Goot, *PLoS One*, 2008, **3**, 1–14.
4. K. Fujita, S. Ishitobi, N. I. Smith, A. Taguchi, Y. Inouye and S. Kawata, *J. Biomed Opt.*, 2009, **14**, 1–7.
5. S. McAughtrie, K. Lau, K. Faulds and D. Graham, *Chem. Sci.*, 2013, **4**, 3566–3572.
6. J. Ando, K. Fujita, N. I. Smith and S. Kawata, *Nano Lett.*, 2011, **11**, 5344–5348.
7. J. Langer, D. J. De Aberasturi, J. Aizpurua, R. A. Alvarez-puebla, B. Auguie, J. J. Baumberg, G. C. Bazan, S. E. J. Bell and A. Boisen, et al., *ACS Nano*, 2020, **14**, 28-117.
8. K. Kneipp, A. S. Haka, H. Kneipp, K. Badizadegan, N. Yoshizawa, C. Boone, K. E. Shafer-Peltier, J. T. Motz, R. R. Dasari, and M. S. Feld, *Appl. Spectrosc.,* 2002, **56**, 150–154.
9. J. Kneipp, H. Kneipp, M. McLaughlin, D. Brown, and K. Kneipp, *Nano Lett.,* 2006, **6**, 2225–2231.
10. H. W. Tang, X. B. Yang, J. Kirkham, and D. A. Smith, *Anal. Chem.,* 2007*,* 79, 3646–3653.
11. K. Huang, K. Bando, J. Ando, N. I. Smith, K. Fujita and S. Kawata, *Methods*, 2014, **68**, 348–353.
12. J. Kneipp, H. Kneipp, B. Wittig and K. Kneipp, *J. Phys. Chem. C*, 2010, **114**, 7421–7426.
13. A. Jaworska, L. E. Jamieson, K. Malek, C. J. Campbell, J. Choo, S. Chlopicki and M. Baranska, *Analyst*, 2015, **140**, 2321–2329.
14. H.-J. Lin, P. Herman and J. R. Lakowicz, *Cytometry*, 2003, **52A**, 77–89.
15. J. Qi, D. Liu, X. Liu, S. Guan, F. Shi, H. Chang, H. He and G. Yang, *Anal. Chem.*, 2015, **87**, 5897–5904.

16. J. Karagiannis and P. G. Young, *J. Cell Sci.*, 2001, **114**, 2929–2941.

17. P. A. Schornack and R. J. Gillies, *Neoplasia,* 2003, **5**, 135–145.

18. P. Paroutis, N. Touret and S. Grinstein, *Physiology*, 2004, **19**, 207–215.

19. J. R. Casey, S. Grinstein and J. Orlowski, *Nat Rev Mol Cell Biol.*, 2009, **11**, 50–61.

20. H. Hou, Y. Zhao, C. Li, M. Wang, X. Xu and Y. Jin, *Sci. Rep.*, 2017, **7**, 1–8.

21. R. J. Aerts, A. J. Durston and W. H. Moolenaar, *Cell*, 1985, **43**, 653–657.

22. A. D. Balgi, G. H. Diering, E. Donohue, K. K. Y. Lam, B. D. Fonseca, M. Numata and M. Roberge, *PLoS One,* 2011, **6**, 21549.

23. A. Taguchi, J. Yu, P. Verma and S. Kawata, *Nanoscale*, 2015, **7**, 17424–17433.

24. P. C. Lee and D. Melsel, *J. Phys. Chem.*, 1982, **86**, 3391–3395.

25. D. R. Ward, N. K. Grady, C. S. Levin, N. J. Halas, Y. Wu, P. Nordlander and D. Natelson, *Nano Lett.*, 2007, **7**, 1396–1400.

26. H. Wang, T. Liu, Y. Huang, Y. Fang, R. Liu, S. Wang and W. Wen, Sci. Rep., 2014, **4**, 1–7.

27. S. H. Wang, C. W. Lee, A. Chiou and P. K. Wei, *J. Nanobiotechnology*, 2010, **8**, 1–33.

28. S. W. Bishnoi, C. J. Rozell, C. S. Levin, M. K. Gheith, B. R. Johnson, D. H. Johnson and N. J. Halas, *Nano Lett.,* 2006, **6**, 1687–1692.

29. V. A. Online, C. Vericat, M. E. Vela, G. Corthey, E. Pensa, G. E. Benitez, P. Carro and R. C. Salvarezza, *RSC Adv.*, 2014, **4**, 27730–27754.

30. K. Hamada, K. Fujita, N. I. Smith, M. Kobayasi, Y. Inouye and S. Kawata, *J. Biomed. Opt.*, 2008, **13**, 1–4.

31. A. F. Palonpon, J. Ando, H. Yamakoshi, K. Dodo, M. Sodeoka, S. Kawata ad K. Fujita, *Nat. Protoc.*, 2013, **8**, 677–962.

32. M. Gu, Z. Heiner and J. Kneipp, *Phys.Chem.Chem.Phys.*, 2015, **17**, 26093–2610.

33. S. Handa, Y. Yu and M. Futamata, *Vib. Spectrosc.*, 2014, **72**, 128–133.

34. T. Itoh, K. Yoshida, V. Biju, Y. Kikkawa, M. Ishikawa and Y. Ozaki, *Phys. Rev. B*,

2007, **76**, 085405-1–5.

35. S. Matsuyama, J. Llopis, Q. L. Deveraux, R. Y. Tsien and J. C. Reed, *Nat. Cell Biol.*, 2000, **2**, 318-32.

36. H. Xu and D. Ren, *Annu Rev Physiol*, 2015, **77**, 57–80.

37. C. Lafourcade, K. Sobo, S. Kieffer-jaquinod, J. 'rome Garin and F. G. van der Goot, *PLoS One*, 2008, **3**, 1–14.

38. M. Schindler, S. Grabski, E. Hoff and S. M. Simon, *Biochemistry*, 1996, **35**, 2811–2817.

39. T. A. Davies, R. E. Fine, R. J. Johnson, C. A. Levesque, W. H. Rathbun, K. F. Seetoo, S. J. Smith, G. Strohmeier, L. Volicer and L. Delva, *Biochem. Biophys. Res. Commun.,* 1993, **194**, 537–543.

40. L. D. Shrode, H. Tapper and S. Grinstein, *J. Bioenerg. Biomembr.*, 1997, **29**, 393–399.

41. M. Miksa, H. Kornura, R. Wu, K. G. Shah and P. Wang, *J. Immunol. Methods,* 2009, **342**, 71–77.

42. D. Perez-Sala, D. Collado-Escobar and F. Mollinedo, *J. Biol. Chem.*, 1995, **270**, 6235–6242.

43. S. Simon, D. Roy and M. Schindler, *Proc. Natl. Acad. Sci. U. S. A.*, 1994, **91**, 1128–1132.

44. S. Hu, C. Zong, K. Lin and X. Wang, *J. Ana. Chem. Soc,* 2018, **140**, 13680–13686.

45. W. Xu, A. Zhao, F. Zuo and J. Hussain, *Anal. Chim. Acta*, 2019, **2**, 100020.

46. S. R. Panikkanvalappil, S. M. Hira, M. A. Mahmoud, M. A. El-Sayed, *J. Am.Chem. Soc.*, 2014, **136**,15961–15968.

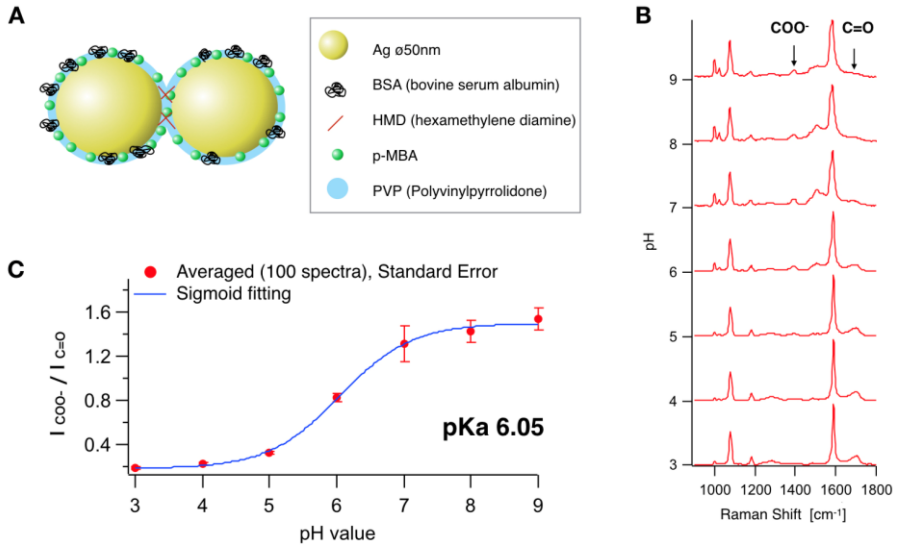

Fig. 1 (A) Schematic of the functionalized Ag nano-assembly (B) SERS spectra of p-MBA on aggregated Ag nanoparticles with HMD conjugation at various pH values from 3.0 to 9.0. Each spectrum is an averaged spectrum (n=100). (C) pH calibration curve obtained by plotting the intensity ratio at 1390 cm^{-1} (COO^-) against 1690 cm^{-1} (C=O). The error bars represent the standard deviation of over 100 different spectra in one-time SERS line scanning imaging. The calibration curve was fitted with a sigmoidal function. The detail experimental condition is written in the material and methods part. The excitation wavelength is 532 nm with 0.3 $mW/\mu m^2$ and the exposure time was 50 ms.

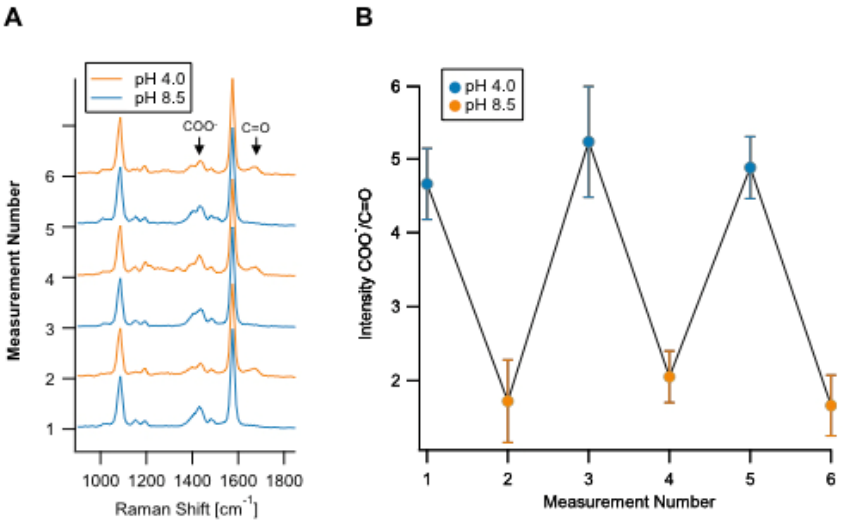

Fig. 2 Repetitive measurement of SERS spectra of p-MBA on aggregated Ag nanoparticles under pH 4.0 and pH 8.5 on the same particles. (A) SERS spectra were collected for 50 spectra and normalized at 1590 cm^{-1} assigned to ring breathing mode. (B) The intensity ratio of the molecular vibrational mode; COO^-/C=O (1390 cm^{-1}/1690 cm^{-1}). The error bar is the standard deviation (n = 50). The excitation wavelength is 532 nm with 0.3 $mW/\mu m^2$ and the exposure time was 50 ms.

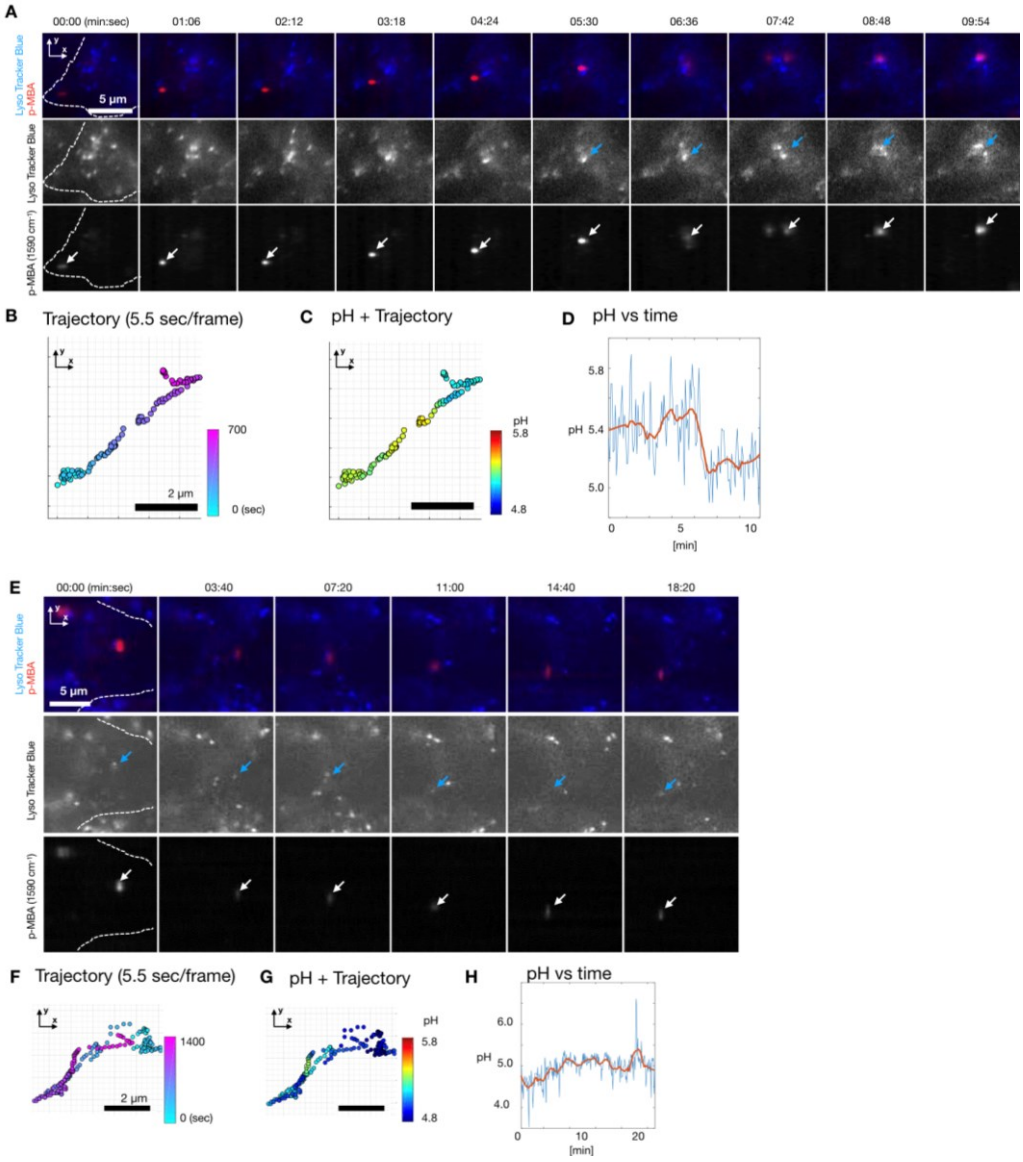

Fig. 3

Time-lapse SERS and fluorescence imaging result of a living HeLa cell. (A, E) Merged image of Lyso Tracker and SERS intensity map at 1590 cm^{-1} (top line), Lyso Tracker (middle line) and SERS intensity map at 1590 cm^{-1}(bottom line) respectively. The images were taken every 5.5 sec interval and displayed every 6 frames for (A) (every 10 frames for (E)). White indicates p-MBA signal from around a targeted nanoparticle and blue indicates the lysosome for each frame. (B, F) Enlarged trajectory of the p-MBA signal at the white area at the bottom line of A, E. The color bar indicates time. The axis is same as A and E respectively. (C, G) Enlarged trajectory of the local pH at the nanoparticle. The color bar indicates pH. The axis is same as A and E respectively. (D, H) Time-course pH change at the white area at the bottom line of A The blue line indicates the raw pH value and the

orange line is smoothed pH (moving average). The laser power was 0.3 mW/μm^2 with 532 nm excitation and the exposure time was 50 ms/line.

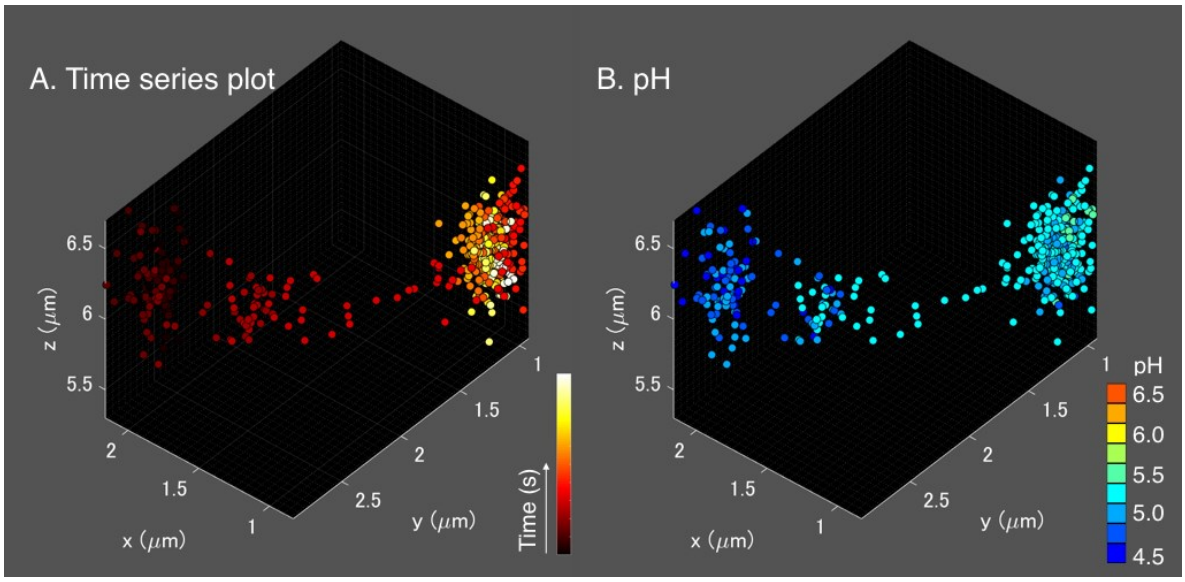

Fig. 4. (A) 3D plot of the nanoparticle trajectory during intracellular transportation in a HeLa cell. The plot consists of 500 data points. The position of the nanoparticle was measured every 200 ms. The color scale represents the time course of the trajectory. (B) 3D plot of the nanoparticle trajectory and pH change during the intracellular transportation in a HeLa cell. The color scale shows the pH value obtained by the SERS intensity ratio of COO^- to C=O. The laser power was 0.3 mW/μm^2 with 532 nm excitation and the exposure time was 50 ms/line.

Supporting Information

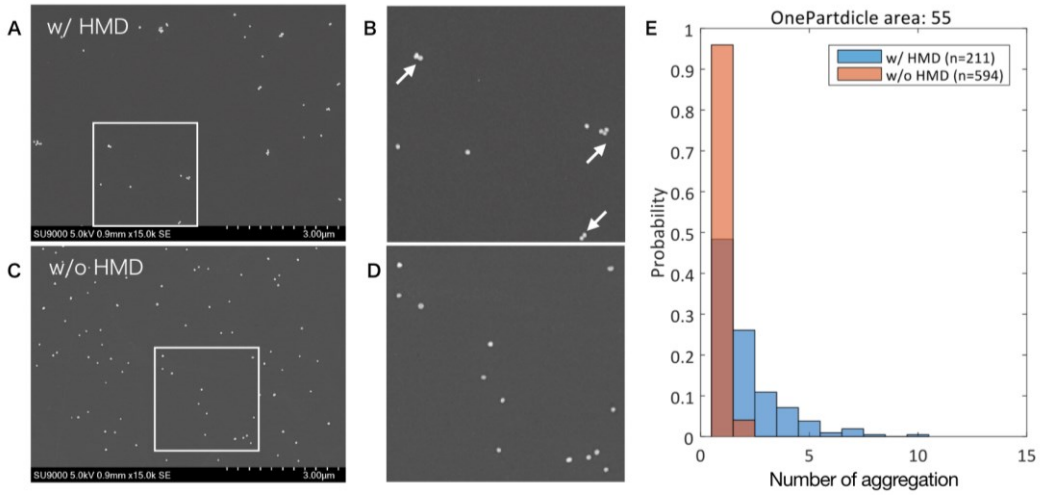

Fig. S1 (A) (B) SEM image of Ag nanoparticles with HMD and (C) (D) without HMD. (B) and (D) are magnified images of the white squares shown in (A) and (C), respectively. The white arrows indicate the aggregated nanoparticles. (E) Histogram of the number of nanoparticles in the aggregates.

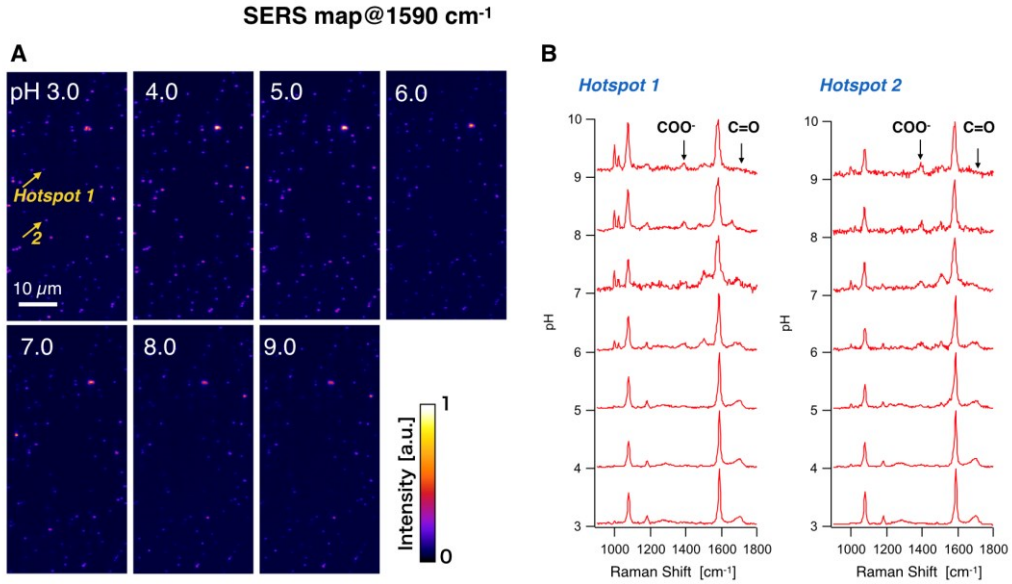

Fig. S2 (A) SERS intensity map at 1590 cm^{-1} with different pH condition at same place. (B) Individual SERS spectra with different pH at allowed in (A).

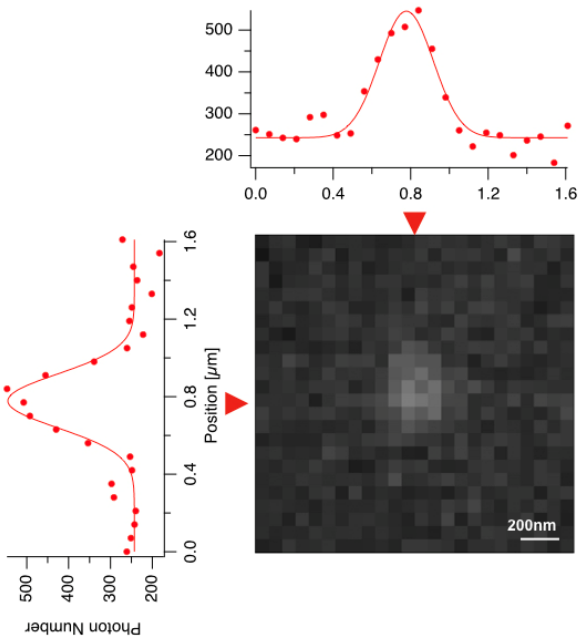

$$\sigma \approx \sqrt{\frac{1}{N}\left(s^2 + \frac{a^2}{12}\right)}$$

Fig. S3 One of the 2D Gaussian fitting of the darkfield image of the nano assembly. Each graph corresponds to the line profile of the indicated position by the triangles and the result of the gaussian fitting. The spatial accuracy was calculated by the shown equation (from Ref. S-1) where N is the number of photons (~250), s is the full width of half-maximum of the spot (~340 nm), and a is the pixel size on the image (70 nm). The position accuracy is ~22 nm.

Reference

S-1 X. Nan, P. A. Sims, P. Chen and X. S. Xie, J. Phys. Chem. B, 2005, 109, 24220–24224.